Author Manuscript

Author Manuscript

Author Manuscript

Author Manuscript

HHS Public Access

Author manuscript

Int J Parasitol. Author manuscript; available in PMC 2019 March 01.

Published in final edited form as:

Int J Parasitol. 2018 March ; 48(3-4): 245–256. doi:10.1016/j.ijpara.2017.09.006.

Cyclopropane fatty acid synthesis affects cell shape and acid resistance in *Leishmania mexicana*

Wei Xu[a,c], **Sumit Mukherjee**[a], **Yu Ning**[a], **Fong-Fu Hsu**[b], and **Kai Zhang**[a,*]

[a]Department of Biological Sciences, Texas Tech University, Lubbock, TX 79409, USA

[b]Mass Spectrometry Resource, Division of Endocrinology, Diabetes, Metabolism, and Lipid research, Department of Internal Medicine, Washington University School of Medicine, St. Louis, MO 63110, USA

Abstract

Cyclopropane fatty acid synthase (CFAS) catalyzes the transfer of a methylene group from *S*-adenosyl methionine to an unsaturated fatty acid, generating a cyclopropane fatty acid (CFA). The gene encoding CFAS is present in many bacteria and several *Leishmania* spp. including *Leishmania mexicana*, *Leishmania infantum* and *Leishmania braziliensis*. In this study, we characterized the CFAS-null and -overexpression mutants in *L. mexicana*, the causative agent for cutaneous leishmaniasis in Mexico and central America. Our data indicate that *L. mexicana* CFAS modifies the fatty acid chain of plasmenylethanolamine (PME), the dominant class of ethanolamine glycerophospholipids in *Leishmania*, generating CFA-PME. While the endogenous level of CFA-PME is extremely low in wild type *L. mexicana*, overexpression of CFAS results in a significant increase. *CFAS*-null mutants (*cfas*$^{-}$) exhibit altered cell shape, increased sensitivity to acidic pH, and aberrant growth in serum-free media. In addition, the CFAS protein is preferentially expressed during the proliferative stage of *L. mexicana* and is required for the cell membrane targeting of lipophosphoglycan. Finally, the maturation and localization of CFAS protein are dependent upon the downstream sequence of the *CFAS* coding region. Without the downstream sequence, the mislocalized CFAS protein cannot fully rescue the defects of *cfas*$^{-}$. Our data suggest that CFA modification of phospholipids can significantly affect the parasite's response to certain adverse conditions. These findings are distinct from the roles of CFAS in *L. infantum*, highlighting the functional divergence in lipid modification among *Leishmania* spp.

Graphical abstract

*Corresponding author: Kai Zhang, Department of Biological Sciences, Texas Tech University, Lubbock, TX 79409, USA. Tel.: +1 806-834-0550. kai.zhang@ttu.edu.

[c]Current address: Department of Molecular Microbiology, Washington University School of Medicine, St. Louis, MO 63110, USA

Publisher's Disclaimer: This is a PDF file of an unedited manuscript that has been accepted for publication. As a service to our customers we are providing this early version of the manuscript. The manuscript will undergo copyediting, typesetting, and review of the resulting proof before it is published in its final citable form. Please note that during the production process errors may be discovered which could affect the content, and all legal disclaimers that apply to the journal pertain.

Note: Supplementary data associated with this article

Author Manuscript Author Manuscript Author Manuscript Author Manuscript

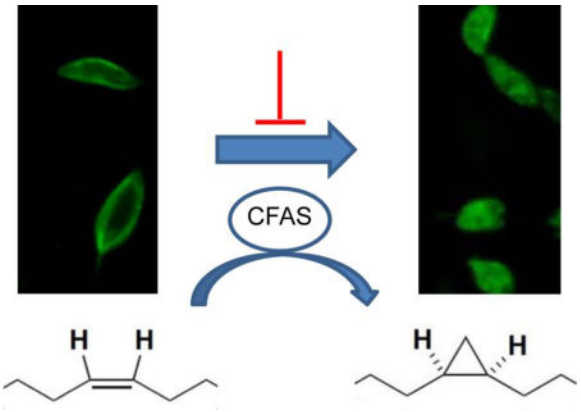

Keywords

Cyclopropane; Plasmalogen; *Leishmania*; Stress response; Lipid; Shape; Acid

1. Introduction

Leishmania parasites are transmitted through the bite of hematophagous sandflies, causing a spectrum of serious diseases (Alvar et al., 2012). During their life cycle, these protozoans alternate between flagellated promastigotes located in the gut of sandflies and non-flagellated amastigotes residing in the phagolysosome of mammalian macrophages. To develop new treatments, it is necessary to understand the molecular strategies utilized by *Leishmania* parasites to survive the harsh conditions in sandflies and humans.

Modification of membrane lipids is a strategy employed by microorganisms to quickly adapt to changing environments (Cronan, 2002; Zhang and Rock, 2008). For example, cyclopropanation of unsaturated fatty acids occurs in the phospholipids of many species of bacteria. In *Escherichia coli*, increased cyclopropane fatty acid (CFA) synthesis is viewed as an adaptive response to low pH (Chang and Cronan, 1999), high temperature and low aeration conditions (Grogan and Cronan, 1997; Chang and Cronan, 1999) . In *Mycobacterium tuberculosis*, cyclopropanation of cell envelope components such as mycolic acids plays a role in modulation of the host innate immune response during infection (Glickman et al., 2000; Rao et al., 2005). CFA synthesis is also implicated in the stress response of *Oenococcus oeni* (Grandvalet et al., 2008) and *Rhodobacter sphaeroides* (Nam et al., 2013). The exact physiological impact of CFA on bacterial membranes remains unclear.

CFA formation is catalyzed by the enzyme cyclopropane fatty acid synthase (CFAS), which transfers a methylene group from S-adenosyl-L-methionine (SAM) to a carbon-carbon double bond within a fatty acyl chain (Supplementary Fig. S1) (Taylor and Cronan, 1979). The *E. coli* CFAS is a soluble enzyme showing activity towards the fatty acids in phosphatidylethanolamine (PE), phosphatidylglycerol and cardiolipin, with PE being the most prominent target (Taylor and Cronan, 1979). Production of *E. coli* CFAS is transiently activated by the RpoS stationary phase sigma factor, followed by proteolytic degradation

Author Manuscript Author Manuscript Author Manuscript Author Manuscript

(Chang et al., 2000). In *Salmonella enterica*, CFAS expression is regulated by small RNA-mediated mRNA stabilization (Frohlich et al., 2013). The labile nature of bacterial CFAS was also observed during purification attempts (Grogan and Cronan, 1984; Taylor and Cronan, 1979).

Among eukaryotes, *CFAS* genes are identified in the genomes of certain plants and trypanosomatids (Bao et al., 2002; Oyola et al., 2012). For *Leishmania* parasites, *CFAS* is present in *Leishmania donovani*, *Leishmania infantum*, *Leishmania braziliensis* and *Leishmania mexicana*, but absent from *Leishmania major*, the causative agent of cutaneous leishmaniasis in the old world (Peacock et al., 2007). In *L. infantum*, CFA constitutes a minor component of the total fatty acid content (<1%) and is mainly found in ethanolamine glycerophospholipids (EGPs) including a family of plasmenylethanolamine (PME) species (Oyola et al., 2012; Hsu et al., 2014). While *L. major* parasites lack CFA, transgenic expression of *L. infantum* CFAS leads to significant production of CFA-containing PME (Oyola et al., 2012; Hsu et al., 2014). Functional analyses of *CFAS*–null mutants in *L. infantum* indicate that CFAS is not required for extracellular parasite growth or phagocytosis by macrophages, but the proline transporter activity appears to be defective in the null parasite (Oyola et al., 2012). Following infection of susceptible mice, *L. infantum CFAS* null mutants show lower parasite burdens in the liver and spleen, but this phenotype cannot be rescued by CFAS re-expression (Oyola et al., 2012). These studies suggest that CFA modification of phospholipids may affect the nutrient uptake and virulence of *L. infantum*. CFA synthesis also seems to contribute to the optimal growth of another trypanosomatid protozoan, *Crithidia fasciculata* (Pascal et al., 1986; Rahman et al., 1988).

Here we characterized the role of CFAS in *L. mexicana*, a species responsible for cutaneous and the rare but serious diffuse cutaneous lesions in humans in Mexico and central America. Similar to *L. infantum*, *L. mexicana* parasites contain a low but detectable level of CFA-modified PME, and the production of CFA-PME is dependent upon CFAS protein expression. Distinct from *L. infantum*, loss of *CFAS* in *L. mexicana* significantly altered parasites' shape and their response to adverse conditions such as acidity and low nutrient levels, but did not affect their virulence. Importantly, the downstream flanking sequence of *CFAS* is crucial for the processing, cellular localization, and full functions of the CFAS protein. Our data suggest that proper expression of CFAS is vital for an optimal response to environmental stress in *L. mexicana*. Thus, CFA modification may have distinct functions among various *Leishmania* spp.

2. Materials and methods

2.1. Materials

1,2-diheptadecanoyl-*sn*-glycero-3-phosphoethanolamine (17:0/17:0-PE) was purchased from Avanti Polar Lipids (Birmingham, AL, USA) as the standard for mass spectrometry analyses. High affinity rat anti-HA-Peroxidase (IgG1) and mouse anti-HA (IgG1) antibodies were purchased from Roche Applied Sciences (Indianapolis, IN, USA). Monoclonal antibodies against *Leishmania* lipophosphoglycan or LPG (CA7AE) and GP63 (mAb #235) were kindly provided by Dr. Stephen Beverley (Washington University School of Medicine, USA) and Dr. Robert McAlister (University of British Columbia, Canada), respectively.

Author Manuscript Author Manuscript Author Manuscript Author Manuscript

Macrophage colony-stimulating factor was purchased from eBioscience Inc (San Diego, CA, USA). All other reagents were purchased from VWR International, USA or Fisher Scientific, USA unless specified otherwise.

2.2. Leishmania culture and growth experiments

Leishmania mexicana M379 (MNYC/BZ/62/M379) wild type (WT) promastigotes were cultivated in M199 medium (pH 7.4) with 10% FBS and other supplements at 26 °C as previously described (Kapler et al., 1990). Cell density was monitored using a hemacytometer. Cell viability was determined by flow cytometry after staining with 5 μg/ml of propidium iodide. To grow axenic amastigotes, *L. mexicana* promastigotes were inoculated in an amastigote medium based on the Drosophila Schneider's medium supplemented with 20% FBS and 0.0015% hemin (pH 5.5) (Bates et al., 1992). Axenic amastigotes were grown in vented flasks in a humidified 32 °C/5% CO_2 incubator.

To examine their tolerance to acidic pH, log phase promastigotes were inoculated into an acidic medium (same composition as the regular M199 medium except the pH was changed to 5.5 or 6.0) and incubated at 26 °C (Xu et al., 2011). To measure cell growth in a FBS-free medium, parasites were inoculated in M199/0.4% BSA (pH 7.4) at 2.0×10^5 cells/ml. Cell density and viability were determined daily.

2.3. Molecular constructs and genetic manipulation

The open reading frame (ORF) of *L. mexicana CFAS* (Trytrypdb ID: LmxM.08.0545) was amplified by PCR from *L. mexicana* genomic DNA and confirmed by sequencing. The resulting 1467 bp DNA fragment was digested with *Bam*HI and cloned into a pXG vector (Ha et al., 1996) and a pXG-GFP+2' vector (Ha et al., 1996) to generate pXG-*CFAS* and pXG-GFP-*CFAS*, respectively. For *CFAS* knock-out constructs, the predicted 5'- and 3'-flanking regions (FRs) were PCR amplified (~1000 bp each) and cloned in tandem into the pUC18 vector. Genes conferring resistance to puromycin (*PAC*) and blasticidin (*BSD*) were then inserted between the 5'- and 3'-FRs to generate pUC-KO-*CFAS*::*PAC* and pUC-KO-*CFAS*::*BSD*, respectively. In addition, the *CFAS* ORF and with its FRs were cloned into the pGEM-phleo-HA' vector (Madeira da Silva et al., 2009) to generate pGEM-phleo-HA-*CFAS* and pGEM-phleo-HA-*CFAS*-3'FR as illustrated in Supplementary Fig. S1E–F. This construct was used to express *CFAS* from its chromosomal locus (Madeira da Silva et al., 2009). Oligo primers used in this study are listed in Supplementary Table S1.

The two *CFAS* alleles in WT parasites were sequentially replaced by *PAC* and *BSD* resistance genes to generate the *cfas*$^-$ mutant (*ΔCFAS*::*PAC* /*ΔCFAS*::*BSD*) (Kapler et al., 1990). To restore CFAS expression, pXG-*CFAS* was introduced into the mutant, and the resulting parasite (resistant to G418) was named *cfas*$^-$/+*CFAS* (*ΔCFAS*::*BSD*/*ΔCFAS*::*PAC*/+pXG-*CFAS*). To restore CFAS expression to near WT level, a *CFAS* chromosomal knock-in was generated by integrating an haemagglutinin (HA)-tagged *CFAS* ORF into the genomic locus of *CFAS* and designated as *cfas*$^-$::*HA-CFAS* (*ΔCFAS*::*PAC*/*ΔCFAS*::*HA-CFAS*) as previously described (Madeira da Silva et al., 2009). To study CFAS localization, pXG-GFP-*CFAS*, pGEM-phleo-HA-*CFAS* or pGEM-phleo-HA-*CFAS*-3'FR were

Author Manuscript Author Manuscript Author Manuscript Author Manuscript

introduced into *cfas*$^{-}$ parasites to generate *cfas*$^{-}$/+*GFP-CFAS*, *cfas*$^{-}$/+*HA-CFAS* or *cfas*$^{-}$/+*HA-CFAS-3'FR*, respectively.

2.4. Lipid analysis by electrospray ionization mass spectrometry (ESI-MS)

Total lipids from log or stationary phase promastigotes were extracted using the Bligh-Dyer method (Bligh and Dyer, 1959). 1,2-diheptadecanoyl-*sn*-glycero-3-phosphoethanolamine (17:0/17:0-PE, FW=720.012, Avanti Polar Lipids) was used as the internal standard to quantify CFA-PME. This standard was added to cell lysates prior to lipid extraction at 1.0×10^7 molecules/cell. EGP species were analyzed by a precursor ion scan of 196 in the negative ion mode using a Thermo Scientific Vantage triple quadrupole mass spectrometer (Zhang et al., 2003). Structural characterization of CFA-PME using low-energy collision induced dissociation (CID) LIT MS^n with high-resolution Fourier transform mass spectrometry (FTMS) was conducted on a Thermo Scientific LTQ Orbitrap Velos mass spectrometer (R=100,000 at *m/z* 400) with Xcalibur operating system as previously described (Hsu et al., 2014). Lipid extract in methanol was loop injected to the ESI source (flow rate: 10 μL/min), where the skimmer was set at ground potential, the electrospray needle was 4.0 kV, and temperature of the heated capillary was set at 300 °C. The automatic gain control of the ion trap was set to 5×10^4, with a maximum injection time of 50 ms. Helium was used as the buffer and collision gas at a pressure of 1×10^{-3} mbar (0.75 mTorr). The MS^n experiments were carried out with an optimized relative collision energy ranging from 25–35% with an activation q value of 0.25 and the activation time of 10 ms to leave a minimal residual abundance of precursor ion (around 20%). The mass selection window for the precursor ions was set at 1 Da wide to admit the monoisotopic ion to the ion-trap for CID for unit resolution detection in the ion-trap or high resolution accurate mass detection in the Orbitrap mass analyzer. Mass spectra were accumulated in the profile mode, typically for 2–10 min for MS^n spectra (n = 2–4).

2.5. Southern blot, western blot and immunofluorescence microscopy

To confirm the genetic manipulation of *CFAS*, genomic DNA from late log phase promastigotes (Fig. 1) was digested with *Sac* I and *Bam*H I, resolved on a 0.7% agarose gel, transferred to a nitrocellulose membrane, and hybridized with [^{32}P]-labeled DNA probes recognizing either a portion of *CFAS* ORF or 5'-flanking region (Supplementary Fig. S2).

To examine the production of LPG and GP63, whole cell lysates or culture supernatants were probed by western blot with either mouse-anti-LPG antibody CA7AE (1:2000), or mouse-anti-GP63 antibody (mAb #235; 1:1000) (Connell et al., 1993), followed by a goat anti-mouse IgG conjugated with horseradish peroxidase (HRP, 1:2000). To detect HA-tagged CFAS, cell lysates were probed with a rat anti-HA IgG-Peroxidase antibody (1:1000). As a loading control, blots were also probed with a 1:5000 mouse anti-α-tubulin antibody. A FluorChem E system (ProteinSimple, San Jose, CA, USA) was used for signal detection and quantitation.

Localizations of LPG and GP63 were determined by immunofluorescence microscopy as previously described (Zhang et al., 2003). Briefly, promastigotes (with and without ethanol permeabilization) were labeled with the CA7AE antibody (1:1000) which recognizes the

Author Manuscript Author Manuscript Author Manuscript Author Manuscript

Gal-Man-phosphate backbone of LPG or an anti-GP63 antibody (from Cedarlane Inc; 1:2000) for 20 min, and then incubated with a goat anti-mouse IgG-FITC (1:1000) antiserum for 20 min. To examine CFAS localization, *cfas*$^{-}$::*HA-CFAS*, *cfas*$^{-}$/+*HA-CFAS*, or *cfas*$^{-}$/+*HA-CFAS-3'FR* cells were labeled with a mouse anti-HA antibody (1:800) and followed by a goat anti-mouse IgG-FITC antiserum (1:1000). *Cfas*$^{-}$/+*HA-CFAS* and *cfas*$^{-}$/+*HA-CFAS-3'-FR* cells were also labeled with a rabbit anti-*Trypanosoma brucei* Bip antibody (1:1000) (Bangs et al., 1993), followed by a goat anti-rabbit IgG-Texas Red (1:2000) antiserum. Hoechst 33342 (1.0 μg/ml) was used to stain DNA for 10 min before microscopy. Images were acquired using an Olympus BX51 Upright Fluorescence Microscope equipped with a digital camera. To quantify the percentage of overlap, 50 cells per group were analyzed for co-localization using Image J JACoP (Just Another Colocalization Plugin) (Bolte and Cordelieres, 2006).

2.6. Macrophage infection and mouse footpad infection

Bone marrow-derived macrophages were obtained from BALB/c mice as previously described (Xu et al., 2011). Macrophage infection was performed using day 3 stationary phase promastigotes at a ratio of five parasites per macrophage (Racoosin and Beverley, 1997).

Footpad infections of BALB/c mice were performed as previously described using metacyclic promastigotes (2×10^5 cells/mouse) or lesion-derived amastigotes (2×10^4 cells/mouse) (Xu et al., 2011). The swelling of footpads (thickness of infected footpad - thickness of uninfected footpad) was measured weekly using a Vernier caliper. Parasite numbers in the infected footpad were determined by limiting dilution assay (Titus et al., 1985).

2.7. Ethics statement

The use of mice in this study was approved by the Animal Care and Use Committee at Texas Tech University, USA (US Public Health Service Approved Animal Welfare Assurance NO. A3629-01). BALB/c mice (female, 8 weeks old) were purchased from Charles River Laboratories International (Wilmington, MA, USA). Mice were housed and cared for in the facility operated by the Animal Care and Resources Center at Texas Tech University, adhering to "Guide for the Care and Use of Laboratory Animals" (the 8th Edition, National Research Council, 2011) for animal husbandry. The facility was inspected monthly and animals were monitored daily by staff members. A complete range of clinical veterinary services was available on a 24 h basis including consultation, diagnostic work-up and clinical care. Laboratory personnel are trained to use proper restraining and injection techniques to reduce pain and distress of animals without compromising the quality of research.

Mice were anesthetized through the peritoneal injection of 100 mg/kg of ketamine hydrochloride and 10 mg/kg of xylazine during recurring procedures including the injection of *Leishmania* parasites into footpads, the recovery of parasites from infected mice, and the measurement of footpad lesion size using a caliper. To reduce potential pain/distress, mice were monitored twice each week for appearance, size, movement and general health condition, and euthanized when the lesions became >2.5 mm or when secondary infections

Author Manuscript Author Manuscript Author Manuscript Author Manuscript

occurred. For the isolation of femur cells and the determination of parasite numbers in the infected footpads, mice were euthanized through CO_2 asphyxiation prior to operations.

2.8. Statistical analysis

The difference between two groups was evaluated by the paired Student's *t* test using Sigmaplot 11.0 (Systat Software Inc, San Jose, CA, USA). *P* values indicating statistical significance were grouped into values of <0.05 and <0.01.

2.9. Nomenclature of lipids

Abbreviations for EGP species (Table 1) were used as previously described (Hsu et al., 2014). For example, the diacyl-PE 1-palmitoyl-2-linoleoyl-*sn*-glycero-3-phosphoethanolamine was designated as 16:0/18:2-PE; the major PME 1-O-octadec-1'-enyl-2-linoleoyl-*sn*-glycero-3-phosphoethanolamine was abbreviated as *p*18:0/18:2-PE; and CFA-PME III 1-O-octadec-1'-enyl-2- (9,10)-methylene-octadecanyl-*sn*-glycero-3-phosphoethanolamine was designated as *p*18:0/C19:0cPro(9)-PE.

3. Results

3.1. Genetic manipulation of CFAS in L. mexicana

Leishmania mexicana CFAS ORF (LmxM.08.0545) is predicted to encode a 55.7 kD protein of 488 amino acids. It contains an SAM-dependent methyltransferase domain (amino acid 185–476) that is conserved in all CFASs (Grogan and Cronan, 1984). No putative signal peptide, transmembrane helices, or organelle-targeting sequences are identified. It shows 80–89% identity to its orthologs in *L. braziliensis*, *L. infantum* and *L. donovani*. It also exhibits 50–54% identity to the *CFAS* orthologs in *M. tuberculosis* and *E. coli*.

To investigate the role of CFAS in *L. mexicana*, *cfas*$^{-}$ *null* mutants were generated through two rounds of targeted gene deletion (Kapler et al., 1990). Southern blot analysis with probes from the upstream flanking region (5'-FR) and the ORF confirmed the loss of *CFAS* in *cfas*$^{-}$ (Fig. 1, Supplementary Fig. S2). The mutant (*cfas*$^{-}$) was complemented with a high copy number plasmid pXG-*CFAS* and the add-back strain was referred to as *cfas*$^{-}$/+*CFAS* (Fig. 1, Supplementary Fig. S2). To restore *CFAS* expression to near WT level, a N-terminally HA-tagged CFAS was introduced into the endogenous locus of *CFAS* to generate the single-allele chromosomal knock-in strain *cfas*$^{-}$::*HA-CFAS* (Madeira da Silva et al., 2009) (Fig. 1, Supplementary Fig. S2). In addition, *cfas*$^{-}$ was also complemented with either *pGEM-HA-CFAS* or *pGEM-HA-CFAS-3'FR*, which contains ~1000 bp of the downstream flanking region following *CFAS*, to generate *cfas*$^{-}$/+*HA-CFAS* or *cfas*$^{-}$/+*HA-CFAS-3' FR*, respectively (Fig. 1, Supplementary Fig. S2).

3.2. Leishmania mexicana CFAS encodes a functional CFAS

Using a precursor ion scan of *m/z* 196 (di-lyso-PE–H_2O) and high resolution FTMS in the negative ion mode, we examined the EGP species in *L. mexicana* promastigotes as deprotonated $[M - H]^{-}$ ions (Fig. 2, Supplementary Fig. S3, Table 1). Similar to other *Leishmania* spp., the majority of EGP in *L. mexicana* belongs to PME (1-O-1'-alkenyl-2-acyl-*sn*-glycero-3-phosphoethanolamine). The most abundant PMEs, detected as the [M - H]

Author Manuscript Author Manuscript Author Manuscript Author Manuscript

$^{-}$ ions, were *p*16:0/18:2-PE at m/z 698.51, *p*18:0/18:2-PE at m/z 726.55, and *p*18:0/18:1-PE at m/z 728.56 (Table 1, Supplementary Fig. S3). Based on their exact molecular masses and CID-MS^2 spectra, $[M - H]^-$ ions at m/z 714.55, 740.56, and 742.58 from WT *L. mexicana* were designated as CFA-PME I (*p*16:0/C19:0cPro[9]-PE), CFA-PME II (*p*18:0/C19:1cPro-PE), and CFA-PME III (*p*18:0/C19:0cPro[9]-PE), respectively (Table 1, Fig. 2). These CFA-containing lipids were of low abundance in WT *L. mexicana* as the combined amount for CFA-PME I, II and III was less than 1% of total EGP in both log phase and stationary phase promastigotes (Table 2, Fig. 2, Supplementary Fig. S3). CFA-PME was nearly undetectable in *cfas*$^{-}$ mutants and the trace amounts of $[M - H]^-$ ions at m/z 714.55, 740.56 and 742.58 likely represented molecular isomers such as EGP species containing odd numbered fatty acyl chains (Tables 1,2, Fig. 2, Supplementary Fig. S3).

Notably, the *cfas*$^{-}$/+*CFAS* add-back parasites contained 14–22 times more cyclopropanated lipids than WT, mainly in the form of CFA-PME III (Fig. 2 E–H, Table 2, Supplementary Fig. S3), presumably due to elevated CFAS expression in these parasites (Fig. 1). An increase in CFA-PME III seemed to coincide with a modest decrease in total PME in *cfas*$^{-}$/+*CFAS* (Table 2). The structure of CFA-PME III (Supplementary Fig. S1) suggests that it is derived from *p*18:0/18:1-PE, one of the main PME species (Table 1, Supplementary Fig. S3). Similar to *cfas*$^{-}$/+*CFAS*, parasites that overexpress GFP-CFAS (*cfas*$^{-}$/+*GFP-CFAS*) or HA-CFAS (*cfas*$^{-}$/+*HA-CFAS* and *cfas*$^{-}$/+*HA-CFAS-3'FR*) also displayed high levels of CFA-PME III (data not shown), indicating that these fusion proteins were functional. In comparison, the CFA-PME level in *cfas*$^{-}$::*HA-CFAS* (the chromosomal knock-in) was close to that in WT parasites (Fig. 2, Table 2, Supplementary Fig. S3). We did not detect any significant changes in *CFAS* null or rescued mutants with respect to other bulk phospholipids such as phosphatidylcholine, inositol phosphorylceramide, or phosphatidylinositol by ESI-MS (data not shown). Collectively, these analyses suggest that i) *L. mexicana* parasites possess a functional CFAS, albeit the endogenous CFA level is quite low; ii) *L. mexicana* CFAS may prefer certain lipid substrates such as *p*18:0/18:1-PE over others; and iii) alternatively, overexpressed CFAS may have more access to *p*18:0/18:1-PE due to the compartmentalization of enzyme or substrates.

3.3. Expression and cellular localization of L. mexicana CFAS

To investigate the expression level of CFAS protein during the promastigote stage, whole cell lysates from *cfas*$^{-}$::*HA-CFAS* parasites were examined by western blot using a HRP linked anti-HA antibody. Two protein bands at 56 kD (the predicted size for HA-CFAS) and 54 kD were detected during the replicative log phase and then gradually disappeared as parasites entered the stationary phase (Fig. 3A). These findings were in line with a previous study using C-terminally myc-tagged CFAS in *L. infantum* (Oyola et al., 2012). Western blots of cell lysates from *cfas*$^{-}$/+*HA-CFAS* and *cfas*$^{-}$/+*HA-CFAS-3'FR* parasites showed a similar growth phase-dependent regulation, even though the HA-CFAS protein was expressed at much higher levels in these parasites (Fig. 3B–C). Curiously, without the 3'-FR, HA-CFAS was mainly found as the larger 56 kD protein (Fig. 3B), yet it was mainly detected at 54 kD when expressed in the presence of 3'-FR (Fig. 3C). Therefore, the 3' untranslated region (UTR) of *CFAS* mRNA may somehow affect the processing or post-translational modification of CFAS protein.

Author Manuscript Author Manuscript Author Manuscript Author Manuscript

We next examined the localization of CFAS in *cfas*$^{-}$/+*HA-CFAS-3'FR* and *cfas*$^{-}$/+*HA-CFAS* parasites by immunofluorescence microscopy. As shown in Fig. 4A, HA-CFAS in *cfas*$^{-}$/+*HA-CFAS-3'FR* (mainly the 54 kD form) displayed a diffuse, punctuated pattern throughout the cell body which was reminiscent of the endoplasmic reticulum (ER); and co-staining with an anti-Bip antibody (ER marker) revealed ~95% overlap (Fig. 4C). In contrast, HA-CFAS in *cfas*$^{-}$/+*HA-CFAS* (mainly the 56 kD form) was primarily detected near the plasma membrane and in intracellular compartments (Fig. 4B); and quantative analysis revealed ~60% overlap with Bip (Fig. 4C). Thus, in addition to post-translational modification, the 3'-FR of *CFAS* ORF also influences the cellular localization of CFAS protein. In agreement with this proposal, an ER-like distribution was detected for HA-CFAS in *cfas*$^{-}$::*HA-CFAS* (HA-CFAS was expressed from the chromosomal locus with the 3'-FR; Supplementary Fig. S4A–C), whereas the GFP-CFAS in *cfas*$^{-}$/+*GFP-CFAS* parasites (without the 3'-FR) was mostly found near the plasma membrane and in the cytoplasm (Supplementary Fig. S4D–F). Together, these findings suggest that the 3'UTR of *CFAS* mRNA (transcribed from the 3'FR) can significantly affect the maturation and targeting of CFAS protein.

3.4. CFAS is required for L. mexicana promastigotes to adapt to certain stress conditions

In *E. coli*, CFAS-mediated membrane modification is implicated in adaptation to changes in pH, temperature, or salinity (Chang and Cronan, 1999). To determine whether CFAS plays similar roles in *L. mexicana*, promastigotes were cultured in either a neutral medium (M199/10% FBS, pH 7.4) or an acidic medium (the same composition as the neutral medium except the pH was adjusted to 5.5 or 6.0). In the neutral medium, *cfas*$^{-}$ promastigotes could survive, proliferate and reach a WT-like maximal density of 3.5–4.0×10^{7} cells/ml in the stationary phase (Supplementary Fig. S5A,B, Fig. 5A). Their growth rate was slightly delayed in comparison to WT, *cfas*$^{-}$/+*CFAS* and *cfas*$^{-}$::*HA-CFAS* parasites (Supplementary Fig. S5A, Fig. 5A). *Cfas*$^{-}$ mutants also appeared more round in shape during the log phase and the stationary phase (Supplementary Fig. S5C–K). This morphological change might reflect altered membrane permeability, cytoskeletal arrangement, or cell polarity control in *cfas*$^{-}$ mutants.

Under acidic conditions (pH 5.5 or 6.0), *cfas*$^{-}$ promastigotes grew slower than WT parasites (Fig. 5B, C). While the chromosomal knock-in (*cfas*$^{-}$::*HA-CFAS*) could restore acid tolerance, the episomal add-back *cfas*$^{-}$/+*CFAS* behaved similarly to *cfas*$^{-}$ mutants (Fig. 5B, C). Thus, the ER-bound, processed form of CFAS may be required for resistance to low pH. We then assessed the ability of *cfas*$^{-}$ mutants to convert into, and grow as, axenic amastigotes in the acidic amastigote medium (pH 5.5) at higher temperatures (Bates et al., 1992). As illustrated in Supplementary Fig. S6, *CFAS* null and overexpression mutants were fully capable of differentiating into non-flagellated axenic amastigotes in culture. Although *cfas*$^{-}$ and *cfas*$^{-}$/+*CFAS* showed slightly longer doubling times than WT and *cfas*$^{-}$::*HA-CFAS*, they were able to reach densities similar to axenic amastigotes (Supplementary Fig. S6A). Thus, the acid resistance defect in *cfas*$^{-}$ promastigotes appears to be transient and does not block the transition into amastigotes.

Author Manuscript Author Manuscript Author Manuscript Author Manuscript

We next examined whether CFAS expression was needed to survive low nutrient conditions by inoculating promastigotes in a neutral, FBS-free M199 medium containing 0.4% BSA (Fig. 6). Under this condition, WT, *cfas*$^{-}$::*HA-CFAS* and *cfas*$^{-}$/+*HA-CFAS-3'-FR* parasites could grow from 1.0 × 10^5 cells/ml to ~5.0 × 10^6 cells/ml in 4 days and their doubling time was almost twice as long in comparison with parasites cultivated in regular medium (M199 with 10% FBS, pH 7.4). After reaching stationary phase in the FBS-free medium, most of these parasites (80–90%) became slender-shaped, metacyclic-like cells (Fig. 6B,C and data not shown). In contrast, *cfas*$^{-}$ mutants were able to reach a much higher density of ~1.1× 10^7 cells/ml in the FBS-free medium, yet 60–80% of these parasites were round in shape in the stationary phase (Fig. 6B, C). Interestingly, *CFAS* add-back parasites without the 3-FR, i.e. *cfas*$^{-}$/+*CFAS* and *cfas*$^{-}$/+*HA*-CFAS, showed intermediate phenotypes in both culture density (~9×10^6 cells/ml at the maximum) and cell shape (40–50% round). Together, these findings suggest that proper expression of the mature form of CFAS is vital for promastigotes to adapt to acidic or nutrient-limiting conditions.

3.5. Dysregulation of CFAS expression affects the production and localization of Glycosylphosphatidylinisotol (GPI)-anchored virulence factors

In *L. major*, ablation of PME synthesis significantly altered the expression of LPG and GP63 (an abundant metalloprotease) which are important virulence factors for promastigotes (Pawlowic et al., 2016). To determine whether cyclopropanation of PME affects the expression of GPI-anchored molecules in *L. mexicana*, we examined the cellular levels of LPG and GP63 by western blot (Supplementary Fig. S7). Clearly, deletion or overexpression of *CFAS* had no significant impact on LPG production (Supplementary Fig. S7A, B). In contrast, the cellular level of GP63 was significantly reduced in *cfas*$^{-}$/+*CFAS* (by 3–5 fold) but not *cfas*$^{-}$ parasites (Supplementary Fig. S7A, C). An increased secretion of proteophosphoglycan (PPG) was also detected in the culture supernatant of *cfas*$^{-}$/+*CFAS* (Supplementary Fig. S7A). Together, these data suggest that CFAS overexpression can negatively affect the biosynthesis of GPI-anchored proteins.

As shown in Fig. 7A, D, LPG was mainly found at the plasma membrane of WT and *cfas*$^{-}$::*HA-CFAS* promastigotes (~94% in cell membrane by quantative analysis; cells were permeabilized with ethanol). In contrast, the same CA7AE antibody detected robust signals from both intracellular locations and the cell surface of membrane-permeabilized *cfas*$^{-}$ mutants (both regular shaped and round cells were included in Fig. 7B). Overall, only ~10% of CA7AE signals were localized in the cell membrane of *cfas*$^{-}$. As a control, only surface-bound LPG was detected in un-permeabilized *cfas*$^{-}$ (Fig. 7C). Since the CA7AE antibody recognizes the Gal-Man-phosphate repeat epitope in LPG, it could detect intermediates of LPG synthesis or other phosphoglycans with the same epitope. These results suggest that *cfas*$^{-}$ mutants fail to compartmentalize the biosynthesis of LPG or LPG-like phosphoglycans.

Localization of GP63 was not affected in CFAS deletion or overexpression parasites (Supplementary Fig. S8). Together, these results indicate that under- or over-production of CFAS may affect the synthesis or proper targeting of GPI-anchored molecules.

Author Manuscript Author Manuscript Author Manuscript Author Manuscript

3.6. Cfas⁻ mutants remain infective in mice and murine macrophages

To study the role of CFAS in virulence, BALB/c mice were infected in the footpad with metacyclic promastigotes of WT, *cfas*⁻, *cfas*⁻/+*CFAS* or *cfas*⁻::*HA-CFAS* (Supplementary Figs. S9A, B). Despite the defects in acid resistance and LPG/GP63 expression, *cfas*⁻ and *cfas*⁻/+*CFAS* parasites induced lesions at similar rates as WT and *cfas*⁻::*HA-CFAS* parasites in mice (Supplementary Fig. S10A). As expected, lesion sizes correlated with parasite burdens (Supplementary Fig. S10B). In addition, no significant difference was detected when the infection was performed using amastigotes isolated directly from mouse footpad lesions (Supplementary Figs. S10C, D). Furthermore, *cfas*⁻ and *cfas*⁻/+*CFAS* parasites were able to invade and survive in bone marrow-derived murine macrophages at very levels as WT promastigotes (Supplementary Fig. S10). Thus, despite its roles in controlling cell shape, acid resistance, and GPI-production, CFAS is not essential for the virulence of *L. mexicana*.

4. Discussion

Our findings suggest that *L. mexicana* CFAS is responsible for the modification of PME into CFA-PME. The endogenous level of CFA-PME is less than 1% of total EGP in WT *L. mexicana*, and largely undetectable in *cfas*⁻ mutants (Fig. 2, Table 1). Despite of its low abundance, CFA-PME appears to play important roles in regulating cell shape and tolerance to low pH (Supplementary Fig. S5, Fig. 5). Loss of CFAS also has a significant impact on the cellular compartmentalization of LPG (Fig. 7), suggesting that the cyclopropanation of PME can affect the physiology of plasma membrane and intracellular organelle membrane.

It is not clear how the trace amount of CFA-PME can exert such a significant impact on a parasite's morphology and membrane property. A molecular dynamics simulation study suggests that CFA can stabilize membranes against adverse conditions while simultaneously promoting their fluidity (Poger and Mark, 2015). Increased production of CFA has been found in association with resistance to miltefosine and amphotericin in *L. infantum* (Fernandez-Prada et al., 2016), suggesting that CFA may change membrane fluidity and permeability. It is also possible that in addition to its PME-modifying activity, CFAS has other targets or possesses non-enzymatic functions. Future work is thus warranted to elucidate the roles of CFA-PME or other targets of CFAS in plasma membrane or other cellular organelles (e.g. ER).

Episomal overexpression of CFAS in *cfas*⁻ results in significant accumulation of CFA-PME (5–25% of total EGP) and a reduced level of PME (Fig. 2, Table 2). This inverse correlation is consistent with the utilization of PME by CFAS as substrates (Supplementary Fig. S1, Table 2). It is not clear why the *cfas*⁻/+*CFAS* parasites contain less GP63 than WT and *cfas*⁻ (Supplementary Fig. S7). Since the post-translational modification of GP63 requires the transfer of a phosphoethanolamine group from an EGP donor to link the protein to a GPI-anchor (Menon et al., 1993), one possibility is that the reduced level of PME (which may serve as the donor) negatively affected the maturation of GP63. Alternatively, the high energy expenditure from CFA-PME production (three molecules of ATPs are required to form one molecule of SAM for CFA synthesis; 2–3 × 10^7 CFA-PME molecules are synthesized in log phase *cfas*⁻/+*CFAS*) (Fish et al., 1981) somehow affected the production

Author Manuscript Author Manuscript Author Manuscript Author Manuscript

of virulence factors such as GP63 which are non-essential for cultured promastigotes. This finding is in line with the observation that *L. infantum* CFAS overexpression in *L. major* attenuates its dermal infection in mice, as described in a previous report (Oyola et al., 2012).

CFAS activity is not required for promastigotes to replicate in the regular medium (M199/10% FBS, pH 7.4) or differentiate into axenic amastigotes (Supplementary Figs. S5, S6). A curious observation is that the *cfas*$^{-}$ mutants fail to transition into metacyclic-like forms when cultured in the FBS-free medium, and instead continue to proliferate as round-shaped cells (Fig. 6). This phenotype suggests loss of a certain sensing mechanism in *cfas*$^{-}$. As cell density increases in the FBS-free medium, WT parasites could sense the depletion of nutrients and respond by ceasing proliferation and starting differentiation. In contrast, *cfas*$^{-}$ mutants fail to detect or transduce the starvation signal, which leads to further replication of undifferentiated cells.

In agreement with a previous study on the *L. infantum* ortholog, *L. mexicana* CFAS protein is only detectable during the log and early stationary phases of promastigotes (Fig. 3). Similar stage-dependent expression is observed when CFAS is overexpressed from high copy number plasmid vectors (Fig. 3), suggesting a robust degradation/post-translational regulation of this protein. This is in agreement with previous studies of *E. coli* CFAS which is highly sensitive to proteolysis (Wang and Cronan, 1994; Chang et al., 2000). The HA-tagged *L. mexicana* CFAS was identified as two protein bands: one at the predicted 56 kD and the other at 54 kD. Our analyses suggest that the immediate downstream sequence of *CFAS* ORF (3'FR) is critical for the processing and/or modification of CFAS protein, as the 56 kD band was mainly generated from pGEM-*HA-CFAS* whereas the 54 kD band was mainly produced from pGEM-*HA-CFAS-3'FR* (Fig. 3). Importantly, the 3'FR is crucial for the ER localization of CFAS and its full functionality, as the *cfas*$^{-}$/+pGEM-*HA-CFAS-3'FR* and *cfas*$^{-}$::*HA-CFAS* parasites showed restored CFA-PME synthesis, cell shape, LPG localization, and proper response to acid and starvation conditions (Figs. 2, 4, 5 and 6). In comparison, the partially mis-localized 56 kD CFAS (from pGEM-*HA-CFAS* and pXG-CFAS) could not fully rescue the defects of *cfas*$^{-}$ in acidic or FBS-free media (Figs. 5, 6), although it was sufficient to complement the deficiency in CFA-PME synthesis and cell shape (Figs. 2, 4, 5 and 6). Thus, the complete ER localization appears to be crucial for the full function of CFAS.

The mechanism of this 3'FR-dependent regulation awaits further investigation. It is well-documented that the 3'-FR (which should be transcribed into 3'UTR) can control mRNA stability and translation efficiency in trypanosomatids, but its effects on protein modification and targeting are relatively understudied (Boucher et al., 2002; McNicoll et al., 2005).

In total, our findings suggest that proper expression of CFAS is important for the fitness of *L. mexicana* parasites under certain environmental stresses such as acidic pH and starvation. These results are quite distinct from previous work on CFAS in *L. infantum*, which is implicated in amino acid uptake and tissue dissemination (Oyola et al., 2012). Thus, CFA-PME may be utilized for different purposes by different *Leishmania* spp., and other species such as *L. major*, which is CFAS null, may possess alternative mechanisms to compensate for the lack of CFAS. Phylogenetic analysis suggests that the *Leishmania* parasites acquired

Author Manuscript Author Manuscript Author Manuscript Author Manuscript

CFAS by horizontal transfer from bacteria (Peacock et al., 2007). In the future, it will be of interest to determine whether CFAS plays a role in *Leishmania* survival and differentiation in the sandfly when parasites must co-habit in the midgut with other microbes.

Supplementary Material

Refer to Web version on PubMed Central for supplementary material.

Acknowledgments

This work was supported by the US National Institutes of Health (AI099380 for KZ and P41-GM103422, P60-DK20579, P30-DK56341 for the Biomedical Mass Spectrometry Resource at Washington University in St. Louis, MO, USA). We thank Dr. Jay Bangs (University at Buffalo, NY, USA), Dr. Stephen Beverley (Washington University School of Medicine, USA) and Dr. W. Robert McMaster (University of British Columbia, Vancouver, Canada) for providing us the rabbit anti-*T. Brucei* Bip antibody, mAb CA7AE and mAb anti-GP63 #235, respectively.

References

Alvar J, Velez ID, Bern C, Herrero M, Desjeux P, Cano J, Jannin J, den Boer M, Team WHOLC. Leishmaniasis worldwide and global estimates of its incidence. PLoS One. 2012; 7:e35671. [PubMed: 22693548]

Bangs JD, Uyetake L, Brickman MJ, Balber AE, Boothroyd JC. Molecular cloning and cellular localization of a BiP homologue in *Trypanosoma brucei*. Divergent ER retention signals in a lower eukaryote. J Cell Sci. 1993; 105(Pt 4):1101–1113. [PubMed: 8227199]

Bao X, Katz S, Pollard M, Ohlrogge J. Carbocyclic fatty acids in plants: biochemical and molecular genetic characterization of cyclopropane fatty acid synthesis of Sterculiafoetida. Proc Natl Acad Sci USA. 2002; 99:7172–7177. [PubMed: 11997456]

Bates PA, Robertson CD, Tetley L, Coombs GH. Axenic cultivation and characterization of *Leishmania mexicana* amastigote-like forms. Parasitology. 1992; 105(Pt 2):193–202. [PubMed: 1454417]

Bligh EG, Dyer WJ. A rapid method of total lipid extraction and purification. Can J Biochem Physiol. 1959; 37:911–917. [PubMed: 13671378]

Bolte S, Cordelieres FP. A guided tour into subcellular colocalization analysis in light microscopy. J Microscopy. 2006; 224:213–232.

Boucher N, Wu Y, Dumas C, Dube M, Sereno D, Breton M, Papadopoulou B. A common mechanism of stage-regulated gene expression in *Leishmania* mediated by a conserved 3'-untranslated region element. J Biol Chem. 2002; 277:19511–19520. [PubMed: 11912202]

Chang YY, Cronan JE Jr. Membrane cyclopropane fatty acid content is a major factor in acid resistance of *Escherichia coli*. Mol Microbiol. 1999; 33:249–259. [PubMed: 10411742]

Chang YY, Eichel J, Cronan JE Jr. Metabolic instability of *Escherichia coli* cyclopropane fatty acid synthase is due to RpoH-dependent proteolysis. J Bacteriol. 2000; 182:4288–4294. [PubMed: 10894739]

Connell ND, Medina-Acosta E, McMaster WR, Bloom BR, Russell DG. Effective immunization against cutaneous leishmaniasis with recombinant bacille Calmette-Guerin expressing the *Leishmania* surface proteinase gp63. Proc Natl Acad Sci USA. 1993; 90:11473–11477. [PubMed: 8265576]

Cronan JE Jr. Phospholipid modifications in bacteria. Curr Opin Microbiol. 2002; 5:202–205. [PubMed: 11934618]

Fernandez-Prada C, Vincent IM, Brotherton MC, Roberts M, Roy G, Rivas L, Leprohon P, Smith TK, Ouellette M. Different Mutations in a P-type ATPase Transporter in *Leishmania* Parasites are Associated with Cross-resistance to Two Leading Drugs by Distinct Mechanisms. PLoS Negl Trop Dis. 2016; 10:e0005171. [PubMed: 27911896]

Author Manuscript Author Manuscript Author Manuscript Author Manuscript

Fish WR, Holz GG Jr, Beach DH, Owen E, Anekwe GE. The cyclopropane fatty acid of trypanosomatids. Mol Biochem Parasitol. 1981; 3:103–115. [PubMed: 7254247]

Frohlich KS, Papenfort K, Fekete A, Vogel J. A small RNA activates CFA synthase by isoform-specific mRNA stabilization. EMBO J. 2013; 32:2963–2979. [PubMed: 24141880]

Glickman MS, Cox JS, Jacobs WR Jr. A novel mycolic acid cyclopropane synthetase is required for cording, persistence, and virulence of *Mycobacterium tuberculosis*. Mol Cell. 2000; 5:717–727. [PubMed: 10882107]

Grandvalet C, Assad-Garcia JS, Chu-Ky S, Tollot M, Guzzo J, Gresti J, Tourdot-Marechal R. Changes in membrane lipid composition in ethanol- and acid-adapted *Oenococcus oeni* cells: characterization of the cfa gene by heterologous complementation. Microbiology. 2008; 154:2611–2619. [PubMed: 18757795]

Grogan DW, Cronan JE Jr. Cloning and manipulation of the *Escherichia coli* cyclopropane fatty acid synthase gene: physiological aspects of enzyme overproduction. J Bacteriol. 1984; 158:286–295. [PubMed: 6325391]

Grogan DW, Cronan JE Jr. Cyclopropane ring formation in membrane lipids of bacteria. Microbiol Mol Biol Rev. 1997; 61:429–441. [PubMed: 9409147]

Ha DS, Schwarz JK, Turco SJ, Beverley SM. Use of the green fluorescent protein as a marker in transfected *Leishmania*. Mol Biochem Parasitol. 1996; 77:57–64. [PubMed: 8784772]

Hsu FF, Kuhlmann FM, Turk J, Beverley SM. Multiple-stage linear ion-trap with high resolution mass spectrometry towards complete structural characterization of phosphatidylethanolamines containing cyclopropane fatty acyl chain in *Leishmania infantum*. J Mass Spectrom. 2014; 49:201–209. [PubMed: 24619546]

Kapler GM, Coburn CM, Beverley SM. Stable transfection of the human parasite *Leishmania major* delineates a 30-kilobase region sufficient for extrachromosomal replication and expression. Mol Cell Biol. 1990; 10:1084–1094. [PubMed: 2304458]

Madeira da Silva L, Owens KL, Murta SM, Beverley SM. Regulated expression of the *Leishmania* major surface virulence factor lipophosphoglycan using conditionally destabilized fusion proteins. Proc Natl Acad Sci USA. 2009; 106:7583–7588. [PubMed: 19383793]

McNicoll F, Muller M, Cloutier S, Boilard N, Rochette A, Dube M, Papadopoulou B. Distinct 3'-untranslated region elements regulate stage-specific mRNA accumulation and translation in *Leishmania*. J Biol Chem. 2005; 280:35238–35246. [PubMed: 16115874]

Menon AK, Eppinger M, Mayor S, Schwarz RT. Phosphatidylethanolamine is the donor of the terminal phosphoethanolamine group in trypanosome glycosylphosphatidylinositols. EMBO J. 1993; 12:1907–1914. [PubMed: 8491183]

Nam TW, Ziegelhoffer EC, Lemke RA, Donohue TJ. Proteins needed to activate a transcriptional response to the reactive oxygen species singlet oxygen. mBio. 2013; 4:e00541–00512. [PubMed: 23300250]

Oyola SO, Evans KJ, Smith TK, Smith BA, Hilley JD, Mottram JC, Kaye PM, Smith DF. Functional analysis of *Leishmania* cyclopropane fatty acid synthetase. PLoS One. 2012; 7:e51300. [PubMed: 23251490]

Pascal RA Jr, Mannarelli SJ, Ziering DL. 10-Thiastearic acid inhibits both dihydrosterculic acid biosynthesis and growth of the protozoan *Crithidia fasciculata*. J Biol Chem. 1986; 261:12441–12443. [PubMed: 3745198]

Pawlowic MC, Hsu FF, Moitra S, Biyani N, Zhang K. Plasmenylethanolamine synthesis in *Leishmania major*. Mol Microbiol. 2016; 101:238–249. [PubMed: 27062077]

Peacock CS, Seeger K, Harris D, Murphy L, Ruiz JC, Quail MA, Peters N, Adlem E, Tivey A, Aslett M, Kerhornou A, Ivens A, Fraser A, Rajandream MA, Carver T, Norbertczak H, Chillingworth T, Hance Z, Jagels K, Moule S, Ormond D, Rutter S, Squares R, Whitehead S, Rabbinowitsch E, Arrowsmith C, White B, Thurston S, Bringaud F, Baldauf SL, Faulconbridge A, Jeffares D, Depledge DP, Oyola SO, Hilley JD, Brito LO, Tosi LR, Barrell B, Cruz AK, Mottram JC, Smith DF, Berriman M. Comparative genomic analysis of three *Leishmania* species that cause diverse human disease. Nat Genet. 2007; 39:839–847. [PubMed: 17572675]

Poger D, Mark AE. A ring to rule them all: the effect of cyclopropane Fatty acids on the fluidity of lipid bilayers. J Phys Chem. B. 2015; 119:5487–5495. [PubMed: 25804677]

Author Manuscript Author Manuscript Author Manuscript Author Manuscript

Racoosin EL, Beverley SM. *Leishmania major*: promastigotes induce expression of a subset of chemokine genes in murine macrophages. Exp Parasitol. 1997; 85:283–295. [PubMed: 9085925]

Rahman MD, Ziering DL, Mannarelli SJ, Swartz KL, Huang DS, Pascal RA Jr. Effects of sulfur-containing analogues of stearic acid on growth and fatty acid biosynthesis in the protozoan *Crithidia fasciculata*. J Medicinal Chem. 1988; 31:1656–1659.

Rao V, Fujiwara N, Porcelli SA, Glickman MS. *Mycobacterium tuberculosis* controls host innate immune activation through cyclopropane modification of a glycolipid effector molecule. J Exp Med. 2005; 201:535–543. [PubMed: 15710652]

Taylor FR, Cronan JE Jr. Cyclopropane fatty acid synthase of *Escherichia coli*. Stabilization, purification, and interaction with phospholipid vesicles. Biochemistry. 1979; 18:3292–3300. [PubMed: 380648]

Titus RG, Marchand M, Boon T, Louis JA. A limiting dilution assay for quantifying *Leishmania major* in tissues of infected mice. Parasite Immunol. 1985; 7:545–555. [PubMed: 3877902]

Wang AY, Cronan JE Jr. The growth phase-dependent synthesis of cyclopropane fatty acids in *Escherichia coli* is the result of an RpoS(KatF)-dependent promoter plus enzyme instability. Mol Microbiol. 1994; 11:1009–1017. [PubMed: 8022273]

Xu W, Xin L, Soong L, Zhang K. Sphingolipid degradation by *Leishmania major* is required for its resistance to acidic pH in the mammalian host. Infect Immun. 2011; 79:3377–3387. [PubMed: 21576322]

Zhang K, Showalter M, Revollo J, Hsu FF, Turk J, Beverley SM. Sphingolipids are essential for differentiation but not growth in *Leishmania*. EMBO J. 2003; 22:6016–6026. [PubMed: 14609948]

Zhang YM, Rock CO. Membrane lipid homeostasis in bacteria. Nat Rev Microbiol. 2008; 6:222–233. [PubMed: 18264115]

Author Manuscript Author Manuscript Author Manuscript Author Manuscript

Highlights

- Cyclopropane fatty acid is a rare but detectable lipid component in *Leishmania mexicana*
- Cyclopropane fatty acid synthase (CFAS) is preferentially expressed during the replicative phase
- The localization of CFAS is regulated by the downstream sequence of the *CFAS* open reading frame
- CFAS-null mutants are viable but show altered morphology and aberrant response to acidic pH and serum deprivation

Author Manuscript Author Manuscript Author Manuscript Author Manuscript

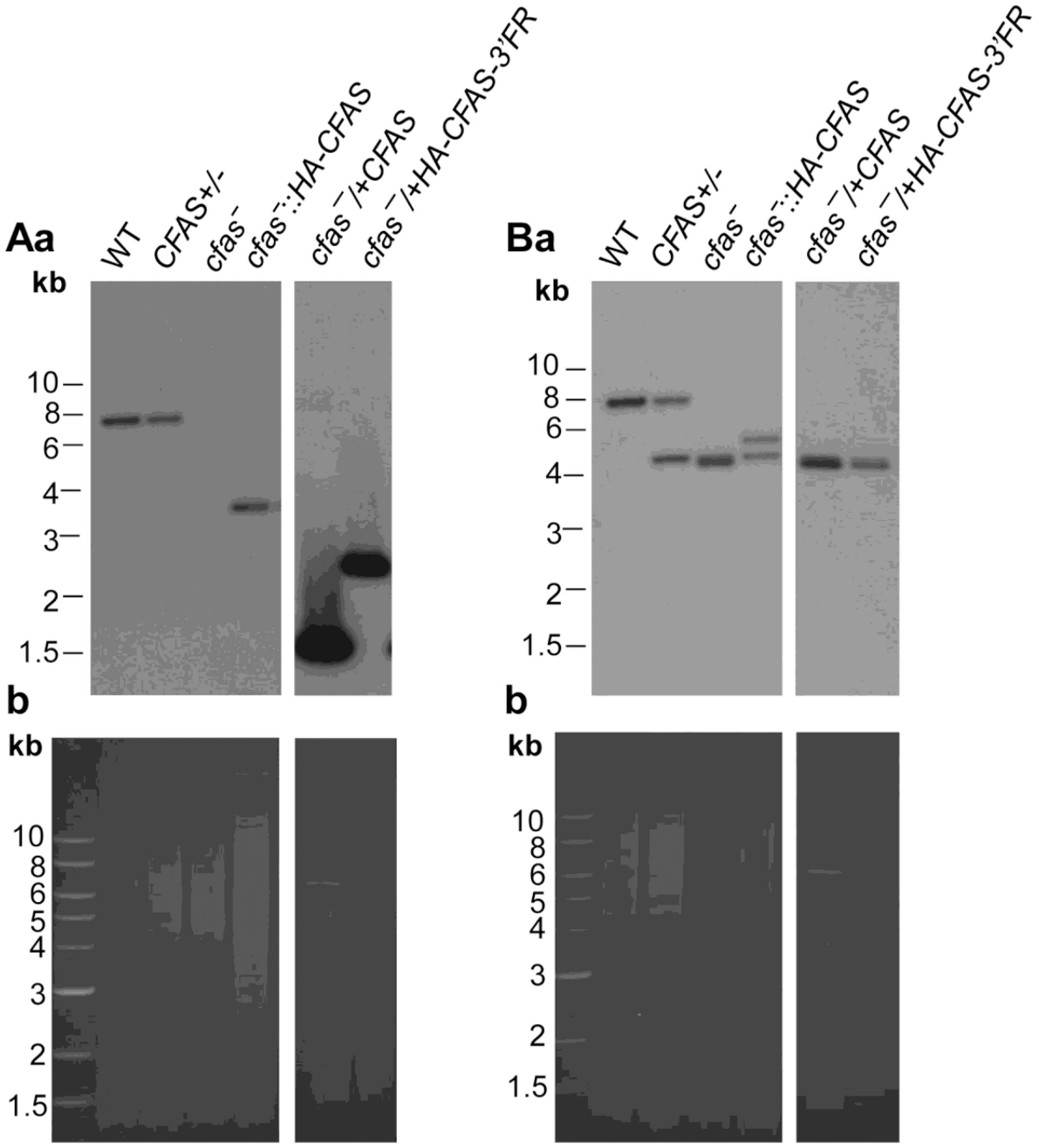

Fig. 1.

Targeted deletion and genetic complementation of Cyclopropane fatty acid synthase (*CFAS*) in *Leishmania mexicana*. Genomic DNA from *L. mexicana* parasites was digested with restriction enzymes and probed with radiolabeled probes from either the open reading frame (ORF) (Aa) or an upstream flanking region (FR) (Ba) of *CFAS*. Ethidium bromide staining of digested DNA is shown (Ab and Bb). DNA fragments corresponding to the *CFAS* locus, its replacements and plasmids (pGEM-HA-CFAS-3'FR for *cfas*$^{-}$/+HA-CFAS-3'FR and pXG-CFAS for *cfas*$^{-}$/+CFAS) were indicated, with more details described in Supplementary Fig. S2. WT, wild type.

Author Manuscript Author Manuscript Author Manuscript Author Manuscript

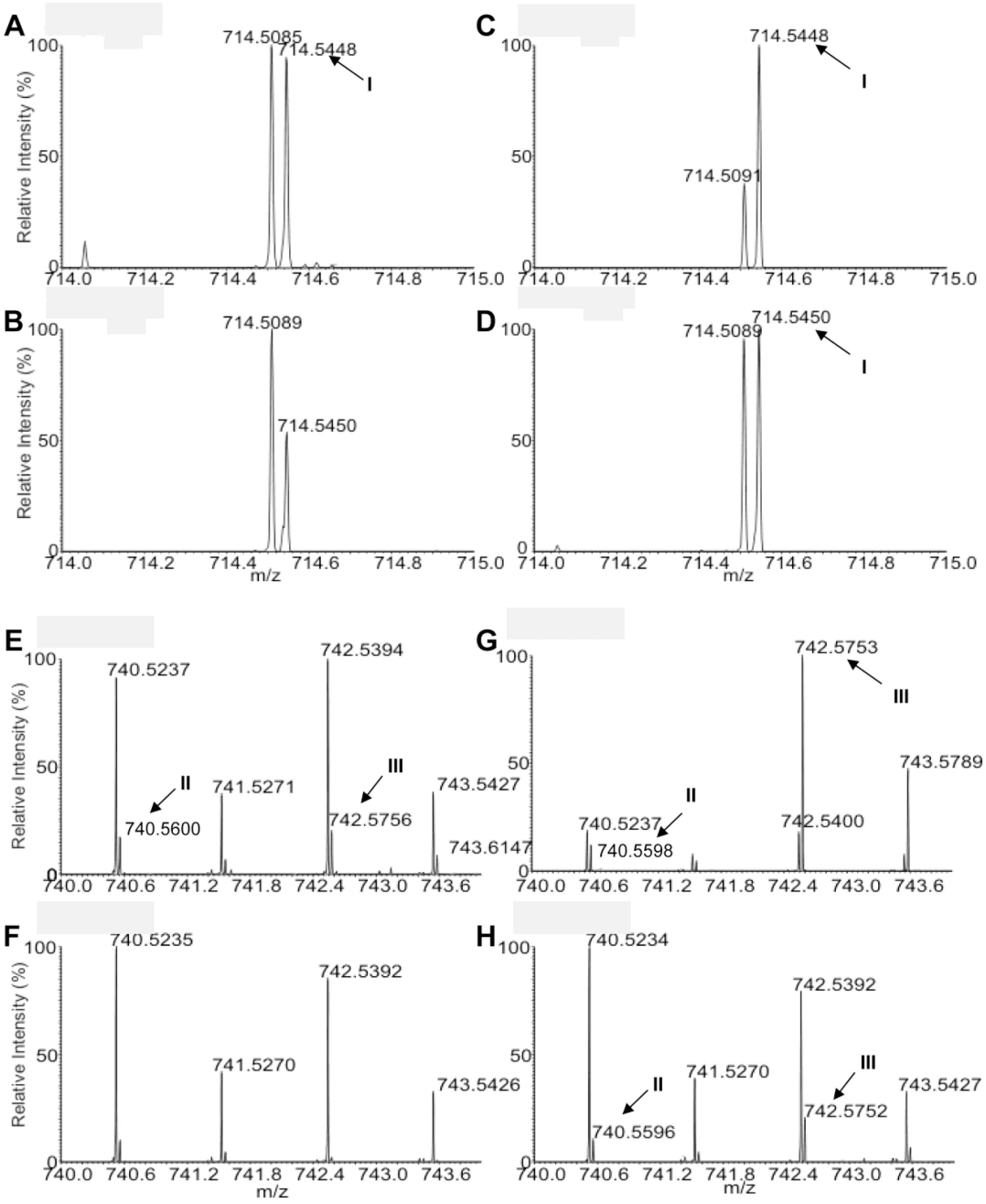

Fig. 2.

Detection of cyclopropane fatty acid (CFA)- plasmenylethanolamine (PME) in *Leishmania mexicana*. Total lipids from log phase promastigotes were analyzed by high resolution electron spray ionization Fourier Transform Mass Spectrometry in the negative ion mode. Mass spectra in the mass range of m/z 714.0–715.0 (A–D) and m/z 740.0–744.0 (E–H) were shown. (A, E) *Leishmania mexicana* wild type (WT); (B, F) *cfas*$^{-}$; (C, G) *cfas*$^{-}$/+*CFAS*; (D, H) *cfas*$^{-}$::*HA-CFAS*. I-III represent the three CFA-PME species detected as [M - H]$^{-}$ ions, which are within 2 ppm deviation of the calculated m/z. I: *p*16:0/C19:0cPro(9)-PE (C40H77O7NP, calculated m/z 714.5443). II: *p*18:0/C19:1cPro-PE (C42H79O7NP,

Author Manuscript Author Manuscript Author Manuscript Author Manuscript

calculated m/z 740.5600). III: *p*18:0/C19:0cPro(9)-PE (C42H81O7NP, calculated m/z 742.5759). In (G), the abundance of III in *cfas*$^{-}$/+*CFAS* is much higher than that of m/z 742.5400 which represents the 18:1/18:1-PE (C41H77O8NP). In contrast, the [M - H]$^{-}$ ions of 18:1/18:1-PE in WT (E), *cfas*$^{-}$ (F), and *cfas*$^{-}$::*HA-CFAS* (H) are more abundant than III. Please note that ions at 741.5270–742.5271, 743.5426–743.5427 and 743.5789 are ^{13}C1-isotopmers.

Author Manuscript Author Manuscript Author Manuscript Author Manuscript

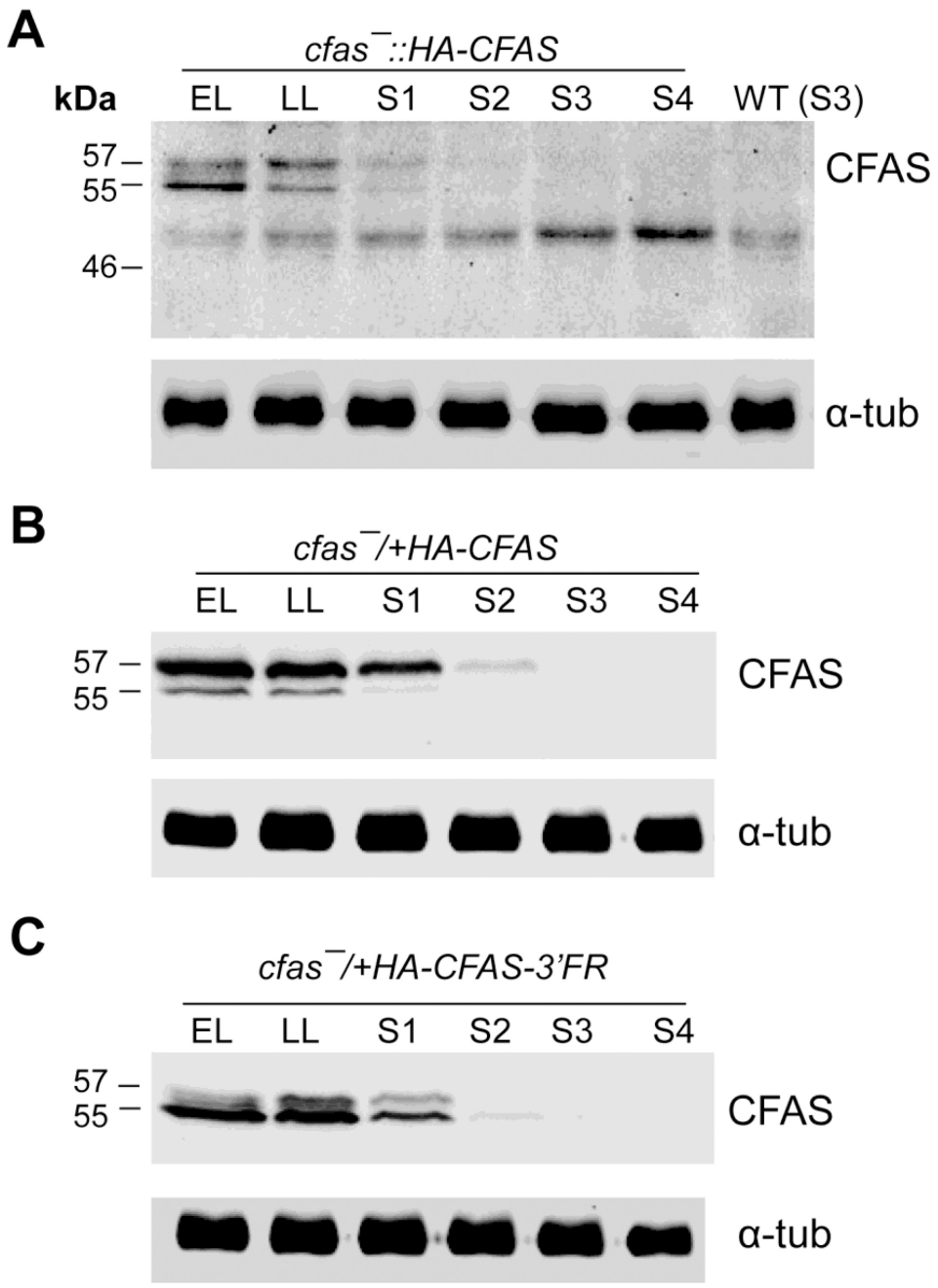

Fig. 3.

Cyclopropane fatty acid synthase (CFAS) protein expression is reduced in stationary phase *Leishmania mexicana* promastigotes. Promastigote lysates from *cfas*⁻::*HA-CFAS* (A), wild type (WT) (A), *cfas*⁻/+*HA-CFAS* (B), and *cfas*⁻/+*HA-CFAS-3'-FR* (C) were analyzed by western blot using a rat anti-HA-Peroxidase antibody or an anti-α-tubulin (α-tub) antibody. EL, early log phase (<1.0 × 10^6 cells/ml); LL, late log phase (6–8 × 10^6 cells/ml); S1-S4, days 1–4 of stationary phase.

Author Manuscript
Author Manuscript
Author Manuscript
Author Manuscript

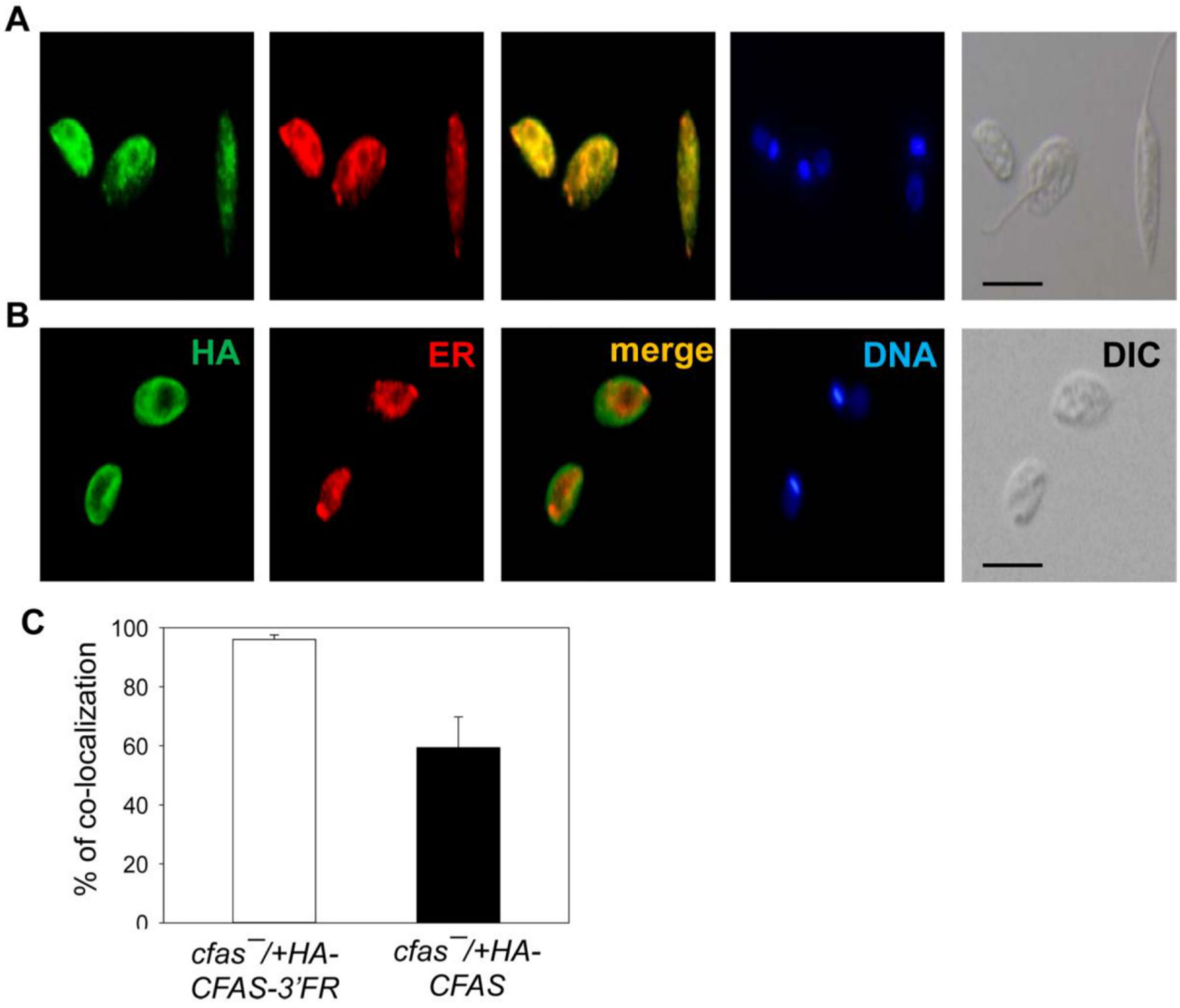

Fig. 4.

Localization of the Cyclopropane fatty acid synthase (CFAS) protein is affected by the downstream flanking sequence (FR) of *CFAS* in *Leishmania mexicana* log phase promastigotes. Log phase promastigotes of *cfas*⁻/+*HA-CFAS-3'FR* (A) and *cfas*⁻/+*HA-CFAS* (B) were permeabilized with ethanol and processed for immunofluorescence microscopy. HA, immuno-staining with a mouse anti-haemagglutinin antibody (1:800), followed by a goat anti-mouse IgG-FITC antiserum (1:1000); ER, immuno-staining with a rabbit anti-*Trypanosoma brucei* Bip antibody, followed by a goat anti-rabbit IgG-Texas Red antiserum; Merge, overlay of HA- and ER-stainings; DNA, Hoechst 33242 staining; DIC, differential interference contrast images. Scale bars =10 μm. (C) Percentages of co-localization between HA-staining and ER-staining were quantified in *cfas*⁻/+*HA-CFAS-3'FR* and *cfas*⁻/+*HA-CFAS* parasites (50 randomly selected cells per group were analyzed) using the Image J JACoP program.

Author Manuscript Author Manuscript Author Manuscript Author Manuscript

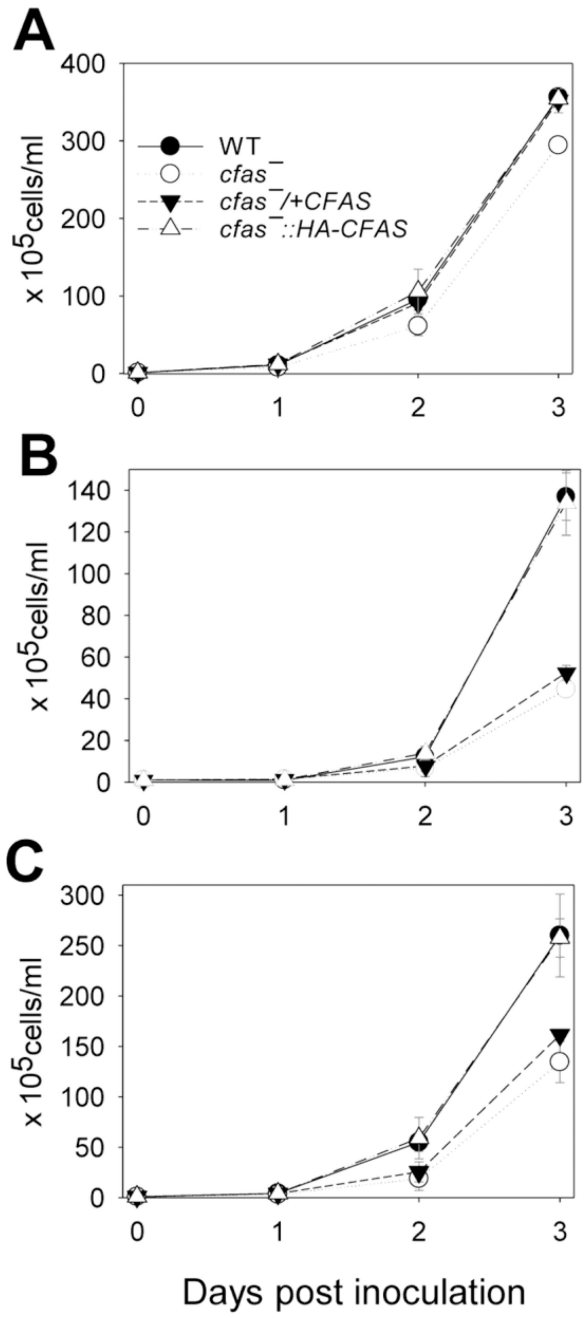

Fig. 5.

Cyclopropane fatty acid synthase mutants (*Cfas*$^{-}$) are sensitive to acidic pH. Log phase *Leishmania mexicana* promastigotes were inoculated in M199/10% FBS media (A, pH 7.4; B, pH 5.5; C, pH 6.0) at 1.0 × 10^5 cells/ml and cultivated for 3 days. Culture densities were determined daily and error bars represent S.D. from three experiments. WT, wild type.

Author Manuscript Author Manuscript Author Manuscript Author Manuscript

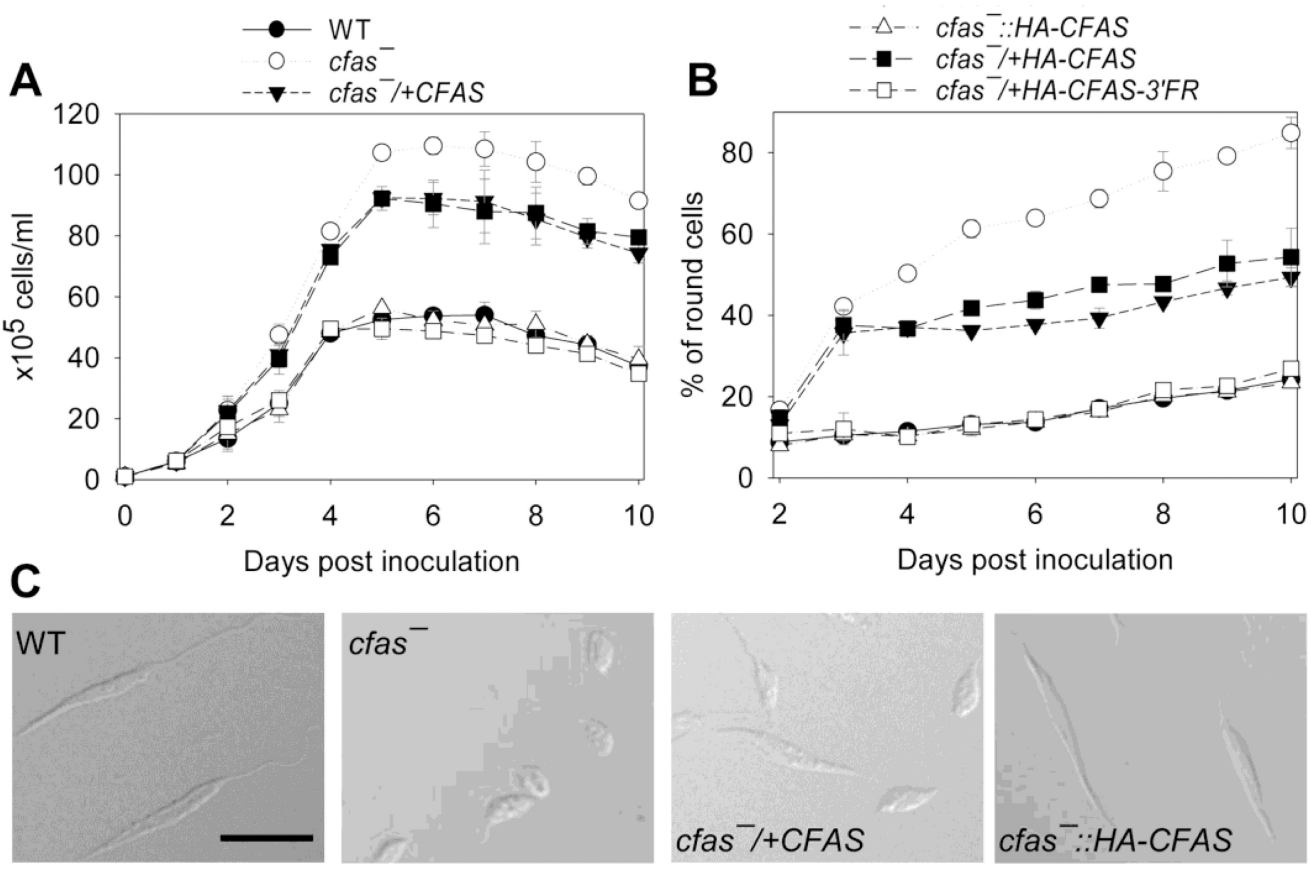

Fig. 6.

Cyclopropane fatty acid synthase mutants (*Cfas*⁻) display aberrant growth in the absence of FBS. Log phase *Leishmania mexicana* promastigotes (●, wild type (WT); ○, *cfas*⁻; ■, *cfas*⁻/+*CFAS*; ▼, *cfas*⁻/+*HA-CFAS*; Δ, *cfas*⁻::*HA-CFA*; □, *cfas*⁻/+*HA-CFAS-3'FR*) were inoculated into FBS-free M199 medium containing 0.4% BSA. The culture density (A) and percentage of round cells (B) were determined daily. Error bars represent S.D. from three experiments. (C) Representative differential interference contrast (DIC) images of day 8 cells (scale bars = 10 μm).

Author Manuscript Author Manuscript Author Manuscript Author Manuscript

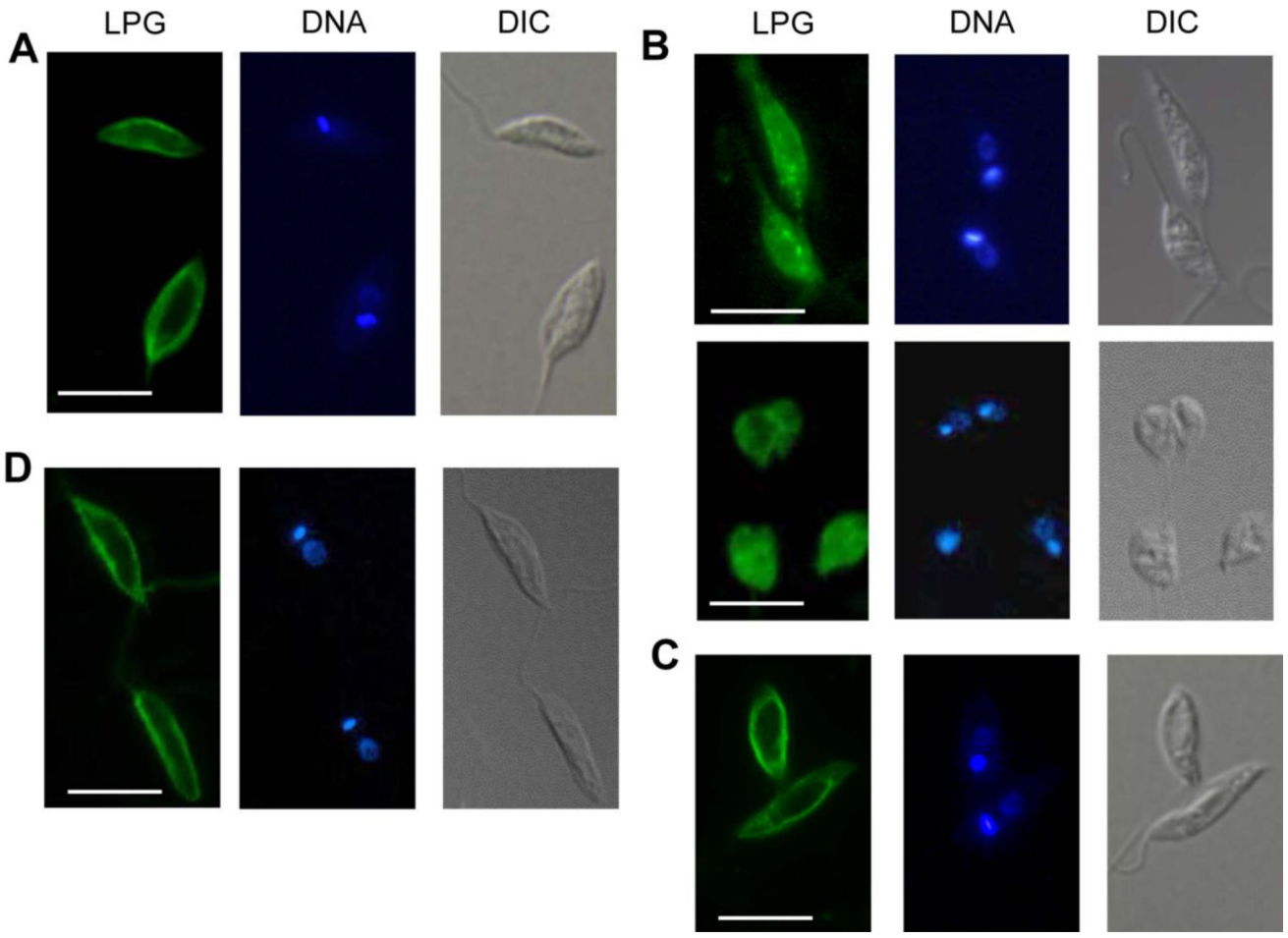

Fig. 7.

Aberrant localization of *Leishmania* lipophosphoglycan (LPG) in Cyclopropane fatty acid synthase mutants (*cfas*$^{-}$). Log phase *Leishmania mexicana* promastigotes of wild type (WT) (A), *cfas*$^{-}$ (B, C), and *cfas*$^{-}$::*HA-CFAS* (D) were analyzed by immunofluorescence microscopy. In (A), (B) and (D), cells were permeablized with 100% ethanol for 10 min on ice, prior to staining with the CA7AE antibody for LPG. In C, *cfas*$^{-}$ parasites were not permeablized. DNA, Hoechst 33242 staining; DIC, differential interference contrast images. Scale bars = 10 μm.

Author Manuscript Author Manuscript Author Manuscript Author Manuscript

Table 1

Major molecular species and relative intensities (Rel.Int.) of ethanolamine glycerophospholipids (EGP) and cyclopropane fatty acid (CFA)- plasmenylethanolamine (PME; [a]) in wild type (WT) *Leishmania mexicana*

m/z of $[M - H]^-$	Rel. Int. (%)	Composition	Structures
698.5135	22	C39 H73 O7 N P	*p*16:0/18:2-PE
700.5290	13	C39 H75 O7 N P	*p*16:0/18:1-PE
714.5089	4.1	C39 H73 O8 N P	16:0/18:2-PE
714.5443 [a]	<1	C40 H77 O7 N P	*p*16:0/C19:0cPro(9)-PE [a], *p*17:0/18:1-PE; *p*18:0/17:1-PE
726.5443	100	C41 H77 O7 N P	*p*18:0/18:2-PE
728.5590	41	C41 H79 O7 N P	*p*18:0/18:1-PE
738.5078	10	C41 H73 O8 N P	18:2/18:2-PE
740.5236	6	C41 H75 O8 N P	18:1/18:2-PE
740.5600 [a]	<1	C42 H79 O7 N P	*p*18:0/C19:1cPro-PE [a], *p*18:0/19:2-PE
742.5399	5	C41 H77 O8 N P	18:0/18:2-PE
742.5759 [a]	<1	C42 H81 O7 N P	*p*18:0/C19:0cPro(9)-PE [a], *p*18:0/19:1-PE

*p*16:0/18:2-PE, 1-O-hexadec-1'-enyl-2-linoleoyl-*sn*-glycero-3-phosphoethanolamine; *p*16:0/18:1-PE, 1-O-hexadec-1'-enyl-2-oleoyl-*sn*-glycero-3-phosphoethanolamine; 16:0/18:2-PE, 1-palmitoyl-2-linoleoyl-*sn*-glycero-3-phosphoethanolamine; *p*16:0/ C19:0cPro(9)-PE, 1-O-hexadec-1'-enyl-2- (9,10)-methylene-octadecanyl-*sn*-glycero-3-phosphoethanolamine; *p*18:0/18:2-PE, 1-O-octadec-1'-enyl-2-linoleoyl-*sn*-glycero-3-phosphoethanolamine; *p*18:0/18:1-PE, 1-O-octadec-1'-enyl-2-oleoyl-*sn*-glycero-3-phosphoethanolamine; 18:2/18:2-PE, 1,2-di-linoleoyl-*sn*-glycero-3-phosphoethanolamine; 18:1/18:2-PE, 1-oleoyl-2-linoleoyl-*sn*-glycero-3-phosphoethanolamine; *p*18:0/ C19:1cPro-PE, 1-O-octadec-1'-enyl-2-methylene-octadecenyl-*sn*-glycero-3-phosphoethanolamine; 18:0/18:2-PE, 1-stearyl-2-linoleoyl-*sn*-glycero-3-phosphoethanolamine; *p*18:0/ C19:0cPro(9)-PE, 1-O-octadec-1'-enyl-2-(9,10)-methylene-octadecanyl-*sn*-glycero-3-phosphoethanolamine.

Author Manuscript

Author Manuscript

Author Manuscript

Author Manuscript

Table 2

Relative abundance of cyclopropane fatty acid (CFA)-plasmenylethanolamine (PME) and PME in *Leishmania mexicana* promastigotes [a]

	WT	*cfas*$^{-}$	*cfas*$^{-}$/+*CFAS*	*cfas*$^{-}$::*HA-CFAS*
CFA-PME (log)	0.116 ± 0.029	0.044 ± 0.014 [b]	2.57 ± 0.74	0.148 ± 0.054
CFA-PME (stat)	0.067 ± 0.014	0.029 ± 0.005[b]	0.94 ± 0.098	0.10 ± 0.025
PME (log)	9.05 ± 2.50	9.33 ± 2.15	8.63 ± 0.82	11.9 ± 3.86
PME (stat)	19 ± 4.55	18.5 ± 8.70	13.4 ± 4.68	17.4 ± 7.53

[a]The abundance of CFA-PME (I+II+III) and PME (*p*18:0/18:2-PE (1-O-hexadec-1'-enyl-2-linoleoyl-*sn*-glycero-3-phosphoethanolamine) + *p*18:0/18:1-PE (1-O-hexadec-1'-enyl-2-oleoyl-*sn*-glycero-3-phosphoethanolamine)) were determined as values relative to a ethanolamine glycerophospholipids (EGP) standard (17:0/17:0-PE) that was added to each sample at 1.0×10^7 molecules/cell before lipid extraction. The relative abundance of the PE standard is set as 1.0. Experiments were performed three times (averages ± S.D.).

[b]The Cyclopropane fatty acid synthase mutants (*cfas*$^{-}$) contain isomers of CFA-PME (Table 1) at low levels.

WT, wild type.